

# Effect of He<sup>3</sup> impurities on the internal friction in crystalline He<sup>4</sup>

V. L. Tsymbalenko

*I. V. Kurchatov Institute of Atomic Energy*

(Submitted 27 December 1985; resubmitted 29 April 1986)

Zh. Eksp. Teor. Fiz. **91**, 934–941 (September 1986)

The amplitude, temperature, and time dependences of the damping constant  $\delta_{\text{He}}$  and modulus of elasticity  $G'$  at 80 kHz are studied for He<sup>4</sup> crystals containing He<sup>3</sup> impurities ( $2 \cdot 10^{-6}$ ,  $10^{-5}$ ,  $2 \cdot 10^{-4}$  at. % He<sup>3</sup>). The introduction of  $10^{-5}$  He<sup>3</sup> causes  $\delta_{\text{He}}$  and  $G'$  to become dependent on the amplitude of the excitation starting at deformations  $\varepsilon_k \sim 10^{-9}$ ; below 0.7 K, the damping constant depends nonmonotonically on the amplitude. The results are analyzed using the Granato-Lukke theory. The parameters of the dislocation lattice, the magnitude of the phonon viscosity, and the binding energy between an impurity and a dislocation are determined. Possible explanations for the anomalously small threshold  $\varepsilon_k$  are considered.

The nature of the defects responsible for the large damping ( $\delta_{\text{He}} \lesssim 0.4$ ) in solid helium<sup>1</sup> at frequencies 10–100 kHz remains unclear. Recent studies<sup>2</sup> using improved apparatus<sup>3</sup> have made it possible to select “good” specimens with reproducible results and to measure the elastic modulus  $G'$  as a function of temperature. In pure specimens,  $\delta_{\text{He}}$  and  $G'$  are both independent of the excitation amplitude for  $\varepsilon = 10^{-9}$ – $10^{-6}$ . The modulus is found to decrease monotonically with cooling, and at the minimum temperature 0.41 K is just  $\sim 20\%$  of its value near the He melting point.

The observed behavior is apparently due to relaxation of structural defects in the internal stress field. Using the relaxation model in Ref. 4 and the measurements in Ref. 2, one concludes that the defects have the following general properties.

1. The behavior is reproducible for “good” specimens—the defect distribution does not change significantly during the experiment.

2. Both  $\delta_{\text{He}}$  and  $G'$  are time-dependent after a thermal shock—the plastic deformation caused by nonuniform heating generates defects that alter the observed relaxation and presumably contribute to the damping.

3. For “good” specimens,  $\delta_{\text{He}}$  has a maximum at  $T = 1.1$  K; the relaxation time is  $\tau_r \approx 5 \cdot 10^{-6}$  s.

4.  $G'$  drops with temperature—there is a decrease in  $\tau_r$  (i.e., an increase in the mobility) with decreasing temperature. Qualitatively, this suggests that the phonon viscosity plays a decisive role in the defect dynamics.

In this paper we study the internal friction in specimens grown from a He<sup>4</sup> +  $x$ He<sup>3</sup> mixture, where  $x = 2 \cdot 10^{-6}$ – $2 \cdot 10^{-4}$ . The addition of the He<sup>3</sup> impurity may give rise to relaxation peaks caused by the diffusion of the He<sup>3</sup> atoms. On the other hand, the impurity may hinder the movement of structural defects by disrupting the regularity of the lattice. The amplitude and temperature dependences in this case can yield qualitative insight by giving information about the way these defects interact with a point defect.

Since the damping and modulus depend on the impurity concentration near a defect,  $\delta_{\text{He}}$  and  $G'$  can serve as measures of the concentration. We are therefore interested in measuring the time behavior for two types of damping—

damping following a temperature jump, and damping after the excitation amplitude is decreased from a large to a small value. Measurements of the first type give information about the relaxation times for the He<sup>3</sup> atoms to reach an equilibrium concentration in the specimen, i.e., on the diffusion of the impurity over distances comparable to the distance between the structural defects. In measurements of the second kind, the distribution of the impurity is disrupted when the excitation causes the defect to oscillate with a large amplitude, whereas for small amplitudes equilibrium is reached through diffusion of the impurity near the defect.

The equipment used previously in Ref. 1 did not permit one to select “good” specimens, and the results there must therefore be regarded as qualitative only.

## EXPERIMENTAL METHOD

The crystalline helium specimens were grown at a constant pressure of  $\sim 35$  atm. The growth vessel and the method for growing and cooling (or heating) the specimens were described previously in Ref. 2. The He<sup>3</sup> content of the gas from which the crystals were grown was given by  $x = 2 \cdot 10^{-6}$ ,  $10^{-5}$ , and  $2 \cdot 10^{-4}$  at. % He<sup>3</sup>. The mixtures were prepared by mixing a known amount of He<sup>3</sup> (He<sup>4</sup> concentration  $\lesssim 0.1\%$ ) with He<sup>4</sup> which had been purified thermomechanically ( $\text{He}^3 < 10^{-6}$ ).

As in the previous experiments, a quartz resonator (torsion fundamental oscillation mode) set up vibrations in the solid helium. The fill factor of the radio-frequency pulse fed to the composite quartz-solid helium vibrator was chosen close to the resonance value  $\sim 80$  kHz. The quality factor  $Q$  and the period  $\tau$  of the composite vibrator were found by analyzing the free decay of the oscillations after the application of a pulse. The measurement technique is discussed in detail in Ref. 2, together with the calculation of the logarithmic damping constant  $\delta_{\text{He}}$  and the mean shearing modulus  $G'$  in terms of  $Q$  and  $\tau$ .

The signal/noise ratio in our experiments was as low as 0.1 at the minimum deformation amplitudes  $\varepsilon \sim 10^{-9}$ . The signal was therefore recorded by a stroboscopic integrator<sup>5</sup> fabricated in conformance with the CAMAC standards. The

data were processed automatically by an AKK-83 crate controller (Ref. 6) containing standard components (registers, D-A converters, timer). The measured signal was processed as follows.

1. The locations of the extrema were determined and the corresponding amplitudes were calculated; the initial and final amplitudes  $\varepsilon_1$  and  $\varepsilon_2$  of the oscillations were found.

2. The method of least squares was used to draw a straight line through the points giving the positions of the extrema, and the mean-square error in the slope was calculated. The slope of this line (equal to the period  $\tau$ ) was used to calculate the modulus  $G'$  averaged over the interval  $(\varepsilon_1, \varepsilon_2)$ . The horizontal bar in Fig. 1b shows a typical interval  $(\varepsilon_1, \varepsilon_2)$ .

3. The oscillation amplitudes were logarithmically smoothed using a 7-point spline approximation and were then differentiated (again with smoothing). We then calculated the dependence  $\delta_{\text{He}}(\varepsilon)$  from the known value of  $\tau$ .

4. The dependence  $\delta_{\text{He}}(\varepsilon)$  and the values  $G'[(\varepsilon_1\varepsilon_2)^{1/2}]$  were then output to a plotter. The entire range of excitation amplitudes  $10^{-9} - 10^{-6}$  was covered by successively decreasing the amplitude of the rf voltage pulse, which was chosen so that the various portions of the  $\delta_{\text{He}}(\varepsilon)$  plot overlapped. The total recording and processing time ranged from 20 s to 10 min, depending on the number of samplings needed per measurement.

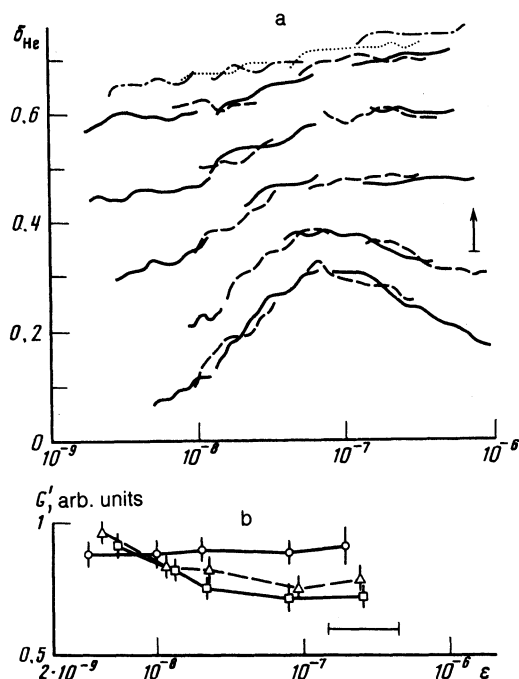


FIG. 1. Damping and elastic modulus in specimens with  $10^{-5}$  at. %  $\text{He}^3$ : a) amplitude dependence of  $\delta_{\text{He}}$  measured at  $T = 1.70, 1.13, 1.03, 0.78, 0.53,$  and  $0.41$  K (top to bottom). The bottom curve is unshifted; each subsequent curve is displaced vertically from the previous one by the amount shown by the arrow. The dotted and dashed-dotted curves at the top and the remaining solid and dashed curves correspond to different excitation amplitudes; b) amplitude dependence of  $G'$ :  $\diamond$ ,  $1.72$  K;  $\triangle$ ,  $0.78$  K;  $\square$ ,  $0.41$  K. The vertical bars give the mean-square error, while the horizontal bar shows a typical  $\varepsilon$  interval in which the period  $\tau$  was measured.

The dependences  $Q(T)$  and  $\tau(T)$  were also recorded continuously on a plotter during the experiment (the design of the measurement block is described in Ref. 3). The damping constant and modulus found by this method correspond to a deformation of  $\sim 10^{-6}$ .

We recorded the time dependence of  $\delta_{\text{He}}$  and  $G'$  in two separate experiments: a) after a step increase in the temperature ( $\tau_1$ ); b) after a step change in the amplitude of the rf excitation pulse ( $\tau_2$ ). In the first series of experiments, the crystal was held below  $0.8$  K to avoid plastic deformation during relaxation. After the amplitude dependences of  $\delta_{\text{He}}$  and  $G'$  were measured, the temperature of the  $\text{He}^3$  bath was changed by  $0.05$ – $0.1$  K. The temperature relaxed after  $\sim 3$  min and was held constant thereafter for  $30$ – $60$  min by an electronic thermostat accurate to  $\sim 2$  mK. We recorded  $\delta_{\text{He}}$  and  $G'$  continuously during the experiment ( $\varepsilon \sim 10^{-9}$ ), and the amplitude dependences were measured at intervals of  $40$ – $200$  s.

In the second series of experiments we studied the time dependence of  $\delta_{\text{He}}$  and  $G'$ : a) after turning on the rf oscillator ( $\varepsilon \sim 10^{-6}$ ) and leaving it on for  $1$  to  $30$  min; b) after decreasing the amplitude of the rf pulse by a factor of  $200$ , so that  $\varepsilon$  ranged from  $\sim 10^{-6}$  to  $\sim 10^{-8}$ . In this series we analyzed the effects of changing the repetition rate of the rf pulses from  $20$  to  $400$  Hz.

## RESULTS

We added  $2 \cdot 10^{-6}$   $\text{He}^3$  to a total of five crystals, and no amplitude dependence of  $\delta_{\text{He}}$  or  $G'$  was detected in this case. The temperature behavior of  $\delta_{\text{He}}$  and  $G'$  was similar to that measured in pure  $\text{He}^4$ .

When the concentration was increased to  $10^{-5}$  (six crystals), both  $\delta_{\text{He}}$  and  $G'$  became amplitude-dependent throughout the range of temperatures and deformations investigated. Some typical results are shown in Fig. 1; the scatter in the values from one specimen to the next is  $\sim 20\%$ . The curves  $\delta_{\text{He}}(\varepsilon)$  are monotonic at high temperature  $T > 0.8$  K but acquire a characteristic maximum at low  $T < 0.8$  K. We note that  $\delta_{\text{He}}$  always depends on  $\varepsilon$ , even at the minimum deformations  $\sim 5 \cdot 10^{-9}$  (see, e.g., the curve at  $0.41$  K). The shearing modulus decreases monotonically as  $\varepsilon$  increases, and the relative magnitude of the drop increases as  $T$  decreases.

The measured temperature dependences of  $G'$  differ for large and small deformations—for  $\varepsilon \sim 10^{-6}$  the curves  $G'(T)$  are the same as for pure  $\text{He}^4$  crystals, while for  $\varepsilon \sim 5 \cdot 10^{-9}$   $G'$  is independent of  $T$  to within the experimental error. Figure 2 shows  $\delta_{\text{He}}(T)$  for the three deformations  $10^{-6}$ ,  $5 \cdot 10^{-8}$ , and  $5 \cdot 10^{-9}$ . We note that the curve for the internal friction, which is independent of the excitation amplitude, lies below the values  $\delta_{\text{He}}(T, \varepsilon = 5 \cdot 10^{-9})$ ; this is because (as noted above) the flat top of the curve was not yet reached at these small deformations. For the same reason,  $\delta_{\text{He}}(T, \varepsilon \rightarrow \infty)$  at low temperatures lies below  $\delta_{\text{He}}(T, \varepsilon = 10^{-6})$ . Taking this into account, we see that  $\delta_{\text{He}}(T, \varepsilon = 10^{-6})$  agrees closely with  $\delta_{\text{He}}(T)$  for pure  $\text{He}^4$ .

Time measurements were carried out by the above techniques for temperatures from  $0.78$  to  $0.52$  K. No time de-

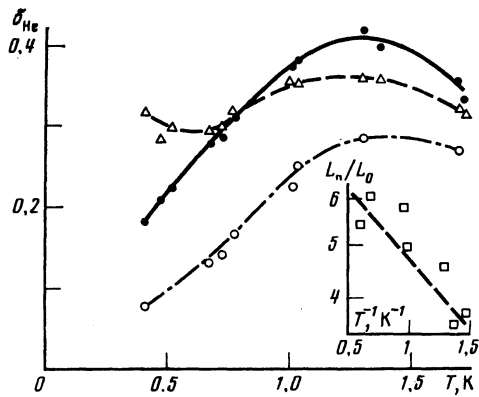


FIG. 2. Temperature dependence of the damping ( $x = 10^{-5}$ ) for three amplitudes:  $\blacklozenge$ ,  $10^{-6}$ ;  $\triangle$ ,  $10^{-7}$ ;  $\diamond$ ,  $5 \cdot 10^{-9}$ . The insert shows how the mean distance between impurities depends on temperature. The dashed line corresponds to an activation energy of 0.6 K.

pendence was detected to within the recording error,  $\tau_1 < 200$  s,  $\tau_2 < 1$  ms.

Figure 3 shows the results for the five crystals with  $x = 2 \cdot 10^{-4}$ . Due to a malfunction in the recording equipment, we were able to measure the amplitude dependence only for the damping constant in the range  $\varepsilon = 10^{-7} - 10^{-6}$ ; the modulus was measured at a fixed amplitude  $10^{-6}$ . Figure 3 shows that increasing the  $\text{He}^3$  content to  $2 \cdot 10^{-4}$  caused  $\delta_{\text{He}}$  to drop. For deformations in the interval  $10^{-7} - 10^{-6}$  the damping constant increased with  $\varepsilon$ ; moreover,  $\delta_{\text{He}}$  decreased with  $1/T$  for both small and large deformations (Fig. 3). In contrast to the situation for pure specimens, here  $G'$  increased as the temperature was lowered.

We were unable to continue measuring  $\delta_{\text{He}}$  at  $\varepsilon = 10^{-7}$  down to the minimum temperature due to beats in the free damping signal. The beating was observed for  $\delta_{\text{He}}(T, \varepsilon) < 0.05$  and was apparently caused by the propagation of an

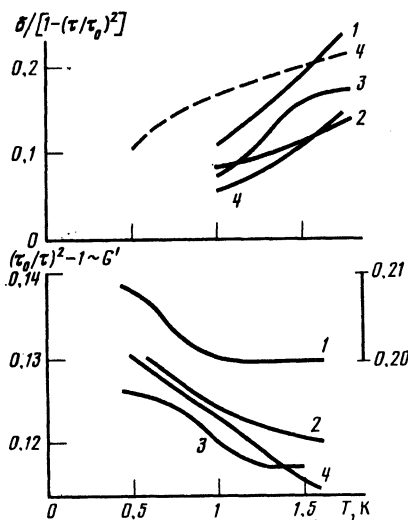


FIG. 3. Temperature curves for the modulus at amplitude  $10^{-6}$  (the right-hand scale is for curve 1) and for the damping; the solid curves show  $\delta_{\text{He}}(T)$  for  $\varepsilon = 10^{-7}$ , while the dashed curve gives  $\delta_{\text{He}}(T)$  for specimen 4 with  $\varepsilon = 10^{-6}$ .

elastic wave from the end faces of the quartz vibrator. This prevented us from carrying out time measurements with a temperature jump; no time dependence of  $\delta_{\text{He}}$  was noted after the deformation amplitude was changed for  $1 \leq T \leq 1.72$  K,  $\tau_2 < 1$  ms.

## DISCUSSION

Figures 1–3 show that a gradual increase in the impurity concentration is reflected in a smooth change in the damping constant and modulus. To within the experimental error, the addition of  $2 \cdot 10^{-6}$  of  $\text{He}^3$  leaves  $\delta_{\text{He}}$  and  $G'$  unchanged. In specimens with  $x = 10^{-5}$ ,  $\delta_{\text{He}}(T)$  and  $G'(T)$  for large  $\varepsilon$  are similar to the curves for pure helium; only the addition of  $2 \cdot 10^{-4}$   $\text{He}^3$  produces a significant (severalfold) drop in the damping at these deformations. We thus conclude that for  $x = 2 \cdot 10^{-6} - 2 \cdot 10^{-4}$ , the primary effect of the  $\text{He}^3$  impurity atoms is to alter the motion of the same defects responsible for damping in pure helium.

The curves  $\delta_{\text{He}}(T)$  do not reveal any new damping peaks associated with the added impurity. Either the relaxation peaks due to  $\text{He}^3$  diffusion lay outside the temperature interval investigated, or else their height was less than the measurement error.

The doped and pure specimens differed qualitatively in that the damping constant and the modulus both depended on the amplitude in the former case. This dependence can be explained by assuming that the  $\text{He}^3$  atoms obstruct the movement of structural defects, and that this effect disappears when the internal stresses are sufficiently large. This model can account qualitatively for the following features of  $\delta_{\text{He}}$  and  $G'$ :

1) At high temperatures  $T \sim T_{\text{melt}}$  (Fig. 1),  $\delta_{\text{He}}$  and  $G'$  are insensitive to the amplitude; the high temperature is sufficient to permit the defects to overcome the impurity barrier;

2) For  $T \approx 0.4$  K the modulus increases with decreasing amplitude; fewer defects can overcome the barrier and trapping occurs at the impurities, so that  $G'$  increases;

3) The temperature dependences of  $\delta_{\text{He}}$  and  $G'(x = 10^{-5})$  (Fig. 2) for  $\varepsilon = 10^{-6}$  are similar to those for pure  $\text{He}^4$ ; the internal stress is so great that the defects easily overcome the barrier and the defect dynamics is governed by the same deceleration mechanism as in pure helium (by the phonon viscosity);

4) The subsequent drop in the damping when  $x$  increases to  $2 \cdot 10^{-4}$  can be explained in two ways: a) if the defect is extended (linear or planar), there will be more impurity stopping sites per defect as the concentration is increased; b) if the number of defects (e.g., for  $x = 10^{-5}$ ) is greater than the number of impurity atoms, increasing  $x$  will increase the number of defects pinned by the impurity;

5) No time dependence of  $\delta_{\text{He}}$  or  $G'$  was observed in the experiments in which the temperature jumped or the excitation amplitude was changed. The  $\text{He}^3$  diffusion rate was thus either so large that the relaxation times were less than the experimental resolution, or else the impurity did not move at all. We observe that in the second case, the change in the amplitude dependences as  $T$  varied implies that the mecha-

nism by which the defects overcome the energy barrier of the impurity must differ at high and low temperatures.

The above conclusions are quite general, since they are based only on the assumption that the damping is due to relaxation. The next step is to identify defects that satisfy the above requirements and have properties 1–4 listed in the Introduction. Little theoretical work has been done on how defects in quantum crystals contribute to mechanical relaxation. Point delocalized defects were considered by Meïerovich,<sup>7</sup> and in a recent paper<sup>8</sup> Markelov solved the problem of determining how a dislocation with delocalized bendings oscillates. Planar defects (grain boundaries, twins, etc.) have not been considered theoretically.

Since point defects (vacancies and impurity atoms) produce damping of magnitude comparable to their concentration,<sup>7</sup> i.e., less than  $10^{-3}$ , they cannot be responsible for the observed relaxation at 80 kHz.

Markelov's formulas<sup>8</sup> for the damping constant at kilohertz frequencies were derived in the delocalized bending model and are valid only for rather high temperatures ( $T \geq 1$  K), for which the mean free path is much less than the length of a segment. The correction to the modulus in pure helium and the effects of an impurity were not considered. Moreover, a comparison of the results in Ref. 2 with the theory<sup>8</sup> does not enable one to unambiguously identify the helium defects as being quantum dislocations. The validity of Markelov's model can be verified qualitatively by measuring the frequency dependence of the damping constant and determining  $\tau_r$  directly. The theory predicts that  $\tau_r \sim T^{-9}$  and  $\delta \sim \tau_r [\omega(1 + \tau_r^2 \omega^2)]^{-1}$ .

In previous papers<sup>1,2</sup> the results have been interpreted using the classical Granato-Lukke (GL) theory for oscillating dislocation segments.<sup>9</sup> This was due partly to the lack of theoretical results on dislocations in quantum crystals, and partly to the close agreement with the predictions of the theory. In the GL model a dislocation is regarded as a line with a mass  $\sim \rho b^2$  per unit length and a tension  $\sim Gb_2$  ( $\rho$  is the density of the material and  $b$  is the Burgers vector); a viscous frictional force  $F = Bv$  per unit length acts on a moving dislocation. The first two results should remain valid for quantum crystals, because the mass depends on the size of the core, while the tension depends on the energy of the deformation field of the dislocation. The constant  $B$  depends on the mechanism by which the vibrational energy of the segment is transferred to the phonon subsystem and may differ markedly from its classical value. An analysis using the GL model for pure He<sup>4</sup> yields the values  $\Omega \Lambda L_0^2 \sim 0.5$ ,  $B = gT^n$ , and  $n = 3$  (here  $\Omega$  is an orientational factor,  $\Lambda$  is the concentration of dislocations, and  $L_0$  is the average length of a segment).

In the GL model an impurity atom interacts with a dislocation with energy  $U_0$ . The rather large stress frees the dislocation from the impurity trap, i.e., there is an amplitude dependence (cf. 1–4 in the Discussion). With increasing temperature it also becomes easier for the dislocations to escape (see 1,2), i.e., the GL model is qualitatively consistent with the observations.

To find the dislocation parameters using the GL theory

we start with the temperature dependences  $\delta_{\text{He}}(T)$  and  $G'(T)$  in the limit of small deformations, for which most of the segments remain pinned by the impurities. The ratio of the damping constants for large and small  $\varepsilon$  (Fig. 2) can be used to calculate the average length  $L(T)$  of a dislocation loop ( $L^{-1} = L_0^{-1} + L_i^{-1}$ , where  $L_i$  is the average distance between impurities). The insert to Fig. 2 shows that  $L_i$  decreases with  $T$ . Setting  $L_i \sim (b/x)\exp(-U_0/T)$ , we get  $L_0 \sim 5 \cdot 10^{-4}$  cm and the estimate  $U_0 \geq 0.6$  K; this gives a lower bound for  $U_0$ , since the amplitude-independent region was not reached even for the minimum deformations  $\sim 5 \cdot 10^{-9}$ . A similar analysis of the data for the specimens with  $2 \cdot 10^{-4}$  He<sup>3</sup> (Fig. 3) gives  $1.2 < U_0 < 2.5$  K.

The above discussion implies that the GL model requires a rather high coefficient for impurity diffusion from the interior toward a dislocation,  $D_1 > L_0^2/\tau_1, D_1 > 10^{-9}$  cm<sup>2</sup>/s.

The GL formulas cannot rigorously be used to analyze the amplitude dependences of  $\delta_{\text{He}}$  and  $G'$ , because the temperature was close to the binding energy and general formulas for the amplitude dependences valid for  $T \sim U_0$  were not obtained. We therefore calculate the critical deformation  $\varepsilon_c \sim U_0/Gb^2L$  sufficient to free a dislocation in specimens with  $x = 10^{-5}$  at the minimum temperature 0.4 K, for which  $\exp(-U_0/T) \sim 10^{-2}$  and the effects of thermal fluctuations may be assumed small. The estimate gives  $L \sim L_0/10$  and  $\varepsilon_c \sim 10^5 - 10^{-4}$ , which is at least three orders of magnitude greater than the observed values (see Fig. 1a). This discrepancy could be due to the following factors: the GL theory may not apply to quantum crystals; in the framework of the GL theory: a) the temperature may not have been low enough to justify neglecting the thermal fluctuations; b) a significant percentage of dislocations may have been freed even at energies less than required to overcome the impurity barrier; c) the longitudinal mobility of He<sup>3</sup> atoms is high, and during the oscillation process they may have moved out toward the edges of a segment, thereby freeing a dislocation without any need to overcome the barrier; then  $D_2 > L_0^2/\tau_2 \sim 10^{-4}$  cm<sup>2</sup>/s. For comparison, at this concentration we have  $D \approx 2 \cdot 10^{-6}$  cm<sup>2</sup>/s in the interior of the crystal.

We may compare the results with the measurements carried out by Iwasa and Suzuki<sup>10</sup> at 10 MHz in specimens with  $3 \cdot 10^{-5}$  He<sup>3</sup> and with the studies of Paalanen *et al.*<sup>11</sup> at 331 Hz,  $x = 3 \cdot 10^{-7}$ ; however, because these frequencies are two orders of magnitude higher and lower than ours, respectively, one cannot rule out the possibility that different types of defects may have been studied in each frequency range. Nevertheless, certain common features are found—the damping in pure helium was large<sup>11</sup>; addition of impurity caused  $\delta_{\text{He}}$  and  $G'$  to depend on the oscillation amplitude<sup>1,10,11</sup>; the damping decreased as the He<sup>3</sup> concentration increased<sup>1,10,11</sup>; the amplitude dependence had a maximum<sup>11</sup>; the values of  $U_0$ ,  $L_0$ , and  $B$  found using the GL theory are similar.

We conclude from our analysis that the available experimental and theoretical results do not suffice to pinpoint the mechanism for the strong damping at kilohertz frequencies. Since the nature of the defects is unclear, it is important

to directly measure the temperature dependence of the relaxation time in pure specimens in order to understand the internal friction processes. (This temperature dependence has hitherto been deduced from  $\delta(T)$  and  $G'(T)$  by using the GL formulas and making assumptions of dubious validity—for example, in a previous paper<sup>2</sup> we assumed that the lengths of the segments were exponentially distributed.) This will require that the frequency dependence of  $\delta$  be measured directly at various temperatures for frequencies 1–100 kHz;  $\tau_r$  can then be deduced from the position of the maximum  $\delta(\omega)$ . The interval 1–100 kHz is chosen to overlap with the other measurements carried out in the kilohertz and low-frequency ranges.

It will be of interest to extend the measurements of  $\delta$  and  $G'$  at 80 kHz down to lower temperatures in order to detect a time dependence. If the same defects are in fact responsible for the observed behavior at MHz and kHz frequencies, one expects that for  $T \sim 100$  mK the damping should depend on the repetition rate of the rf pulses and have typical relaxation times 20–40 ms, as was found by Iwasa and Suzuki.<sup>10</sup> At lower temperatures  $\sim 20$  mK, time dependences with relaxation periods  $\sim 1$  h may be observed (Paalanen *et al.*<sup>11</sup>).

I am deeply grateful to A. N. Sytin, G. A. Dantsevich, and A. V. Ekimov for providing the AKK-83 crate controller and for technical advice and programming assistance.

I would also like to thank V. G. Brovchenko, Yu. A. Karzhavin, V. S. Pavlov, and S. M. Khodov for their support, for valuable technical consultations, and for providing software. Finally, I am grateful to I. A. Gachechiladze, D. V. Pavlov, and A. V. Merkelov for their interest in this work and for fruitful discussions.

<sup>1</sup>V. L. Tsymbalenko, Zh. Eksp. Teor. Fiz. **74**, 1507 (1978) [Sov. Phys. JETP **47**, 787 (1978)].

<sup>2</sup>V. L. Tsymbalenko, Zh. Eksp. Teor. Fiz. **87**, 943 (1984) [Sov. Phys. JETP **60**, 537 (1984)].

<sup>3</sup>V. I. Voronin and V. L. Tsymbalenko, Prib. Tekh. Eksp. No. 4, 197 (1983).

<sup>4</sup>A. S. Nowick and B. S. Berry, *Anelastic Relaxation in Crystalline Solids*, Academic Press, New York (1972).

<sup>5</sup>M. V. Borisov and V. L. Tsymbalenko, Prib. Tekh. Eksp. No. 3, 146 (1984).

<sup>6</sup>G. A. Dantsevich, A. V. Ekimov, and A. N. Sytin, Inst. Fiz. Vys. Energ. Preprint No. 84-41, Serpukhov (1984).

<sup>7</sup>A. E. Meierovich, Zh. Eksp. Teor. Fiz. **67**, 744 (1974) [Sov. Phys. JETP **40**, 368 (1974)].

<sup>8</sup>A. V. Markelov, Zh. Eksp. Teor. Fiz. **88**, 205 (1985) [Sov. Phys. JETP **61**, 118 (1985)].

<sup>9</sup>A. Granato and E. Lücke, *Physical Acoustics*, Vol. 4, Part A [Russian translation], Mir, Moscow (1969), p. 261.

<sup>10</sup>I. Iwasa and H. Suzuki, J. Phys. Soc. Jpn. **49**, 1722 (1980).

<sup>11</sup>M. A. Paalanen, D. J. Bishop, and H. W. Dail, Phys. Rev. Lett. **46**, 664 (1981).

Translated by A. Mason